REPORT DOCUMENTATION PAGE

Form Approved
OMB No. 0704-0188

1. REPORT DATE *(DD-MM-YYYY)*	2. REPORT DATE	3. DATES COVERED *(From - To)*
	June 25, 2001	Interim Report

4. TITLE AND SUBTITLE

Design and Synthesis of Inorganic/Organic Hybrid Microstructures

5a. CONTRACT NUMBER

5b. GRANT NUMBER

N00014-93-1-0245

5c. PROGRAM ELEMENT NUMBER

PR No: 01PR0086-00

6. AUTHOR(S)

John H. Harreld, Bruce Dunn and Linda F. Nazar

5d. PROJECT NUMBER

5e. TASK NUMBER

5f. WORK UNIT NUMBER

7. PERFORMING ORGANIZATION NAME(S) AND ADDRESS(ES)

Bruce S. Dunn
Department of Materials Science and Engineering
University of California, Los Angeles
Los Angeles, CA 90095

8. PERFORMING ORGANIZATION REPORT NUMBER

Technical Report #15

9. SPONSORING/MONITORING AGENCY NAME(S) AND ADDRESS(ES)

Office of Naval Research
800 North Quincy Street
Arlington, VA 22217

12. DISTRIBUTION AVAILABILITY STATEMENT

Reproduction in whole, or in part, is permitted for any purpose of the United States Government.
This document has been approved for public release and sale; its distribution is unlimited.

13. SUPPLEMENTARY NOTES

Published in: *International Journal of Inorganic Materials*

14. ABSTRACT

Vanadium oxide/polypyrrole (V_2O_5/PPy) hybrid aerogels were prepared using three different strategies. These approaches were focused on either sequential or consecutive polymerization of the inorganic and organic networks. The hybrid microstructure differed greatly depending on which synthesis approach was used. When the inorganic and organic precursors were allowed to polymerize simultaneously, the resulting gels exhibited a nanometer scaled microstructure with a homogeneous distribution of the PPy and the V_2O_5. Through this route, a suitable microstructure and composition for a lithium secondary battery cathode were obtained. For the full benefit of the PPy phase to be achieved, a suitable doping procedure is still required to oxidize the PPy into its high conductivity state while preserving the inorganic structure.

15. SUBJECT TERMS

vanadium oxide, aerogel, inorganic/organic material, electrochemical properties

16. SECURITY CLASSIFICATION OF:			17. LIMITATION OF ABSTRACT	18. NUMBER OF PAGES	19a. NAME OF RESPONSIBLE PERSON
a. REPORT	b. ABSTRACT	c. THIS PAGE			19b. TELEPONE NUMBER *(Include area code)*
U	U	U		31	

Standard Form 298 (Rev. 8-98)
Prescribed by ANSI-Std Z39-18

OFFICE OF NAVAL RESEARCH

GRANT: N00014-93-1-0245
R&T Code: 4133041
PR Number: 01PR00860-00

Dr. Richard Carlin

Technical Report #15

Design and Synthesis of Inorganic/Organic Hybrid Microstructures

By

John H. Harreld, Bruce Dunn and Linda F. Nazar*

Published in:
International Journal of Inorganic Materials

Department of Materials Science and Engineering
University of California, Los Angeles
Los Angeles, CA 90095-1595

* Department of Chemistry
University of Waterloo
Waterloo, Ontario, Canada

June 25, 2001

Design and Synthesis of Inorganic/Organic Hybrid Microstructures

J. H. Harreld*, B. Dunn*, and L. F. Nazar**
* Department of Materials Science and Engineering,
University of California, Los Angeles,
Los Angeles, CA 90095-1595
** Department of Chemistry, University of Waterloo,
Waterloo, Ontario, Canada

ABSTRACT

Vanadium oxide/polypyrrole (V_2O_5/PPy) hybrid aerogels were prepared using three different strategies. These approaches were focused on either sequential or consecutive polymerization of the inorganic and organic networks. The hybrid microstructure differed greatly depending on which synthesis approach was used. Microcomposite aerogels were synthesized by encapsulating a dispersion of preformed PPy in a V_2O_5 gel. In the second approach, pyrrole was polymerized and doped within the pore volume of a preformed V_2O_5 gel. The hybrid microstructure of these materials was nanometer scaled but inhomogeneous. When the inorganic and organic precursors were allowed to polymerize simultaneously, the resulting gels exhibited a nanometer scaled microstructure with a homogeneous distribution of the PPy and the V_2O_5. Through this route, a suitable microstructure and composition for a lithium secondary battery cathode were obtained. Undoped material with a composition of $[PPy]_{0.8}V_2O_5$ exhibited a lithium intercalation capacity comparable to that of V_2O_5 aerogel. For the full benefit of the PPy phase to be achieved, a suitable doping procedure is still required to oxidize the PPy into its high conductivity state while preserving the inorganic structure.

1. INTRODUCTION

The synthesis of inorganic/organic hybrid materials has received considerable attention in the past several years because of the prospect of developing materials with unique microstructures and properties [1,2]. The interest in such materials is that with the large number of chemical and structural modifications available, it is possible to design specific properties and produce novel materials with both inorganic and organic characteristics. Advanced materials derived according to these principles have applications in many areas such as optics, electrochemistry, mechanics, electronics, and biology. The synthesis of inorganic/organic hybrid materials is made more versatile by sol-gel chemistry. Sol-gel techniques allow

inorganic materials to be synthesized at low temperatures without the degradation of organic functional groups or polymers. The solution nature of the sol-gel process leads to molecular level mixing and the production of nanostructured materials.

The combination of conducting polymers with transition metal oxides is of substantial interest and the synthesis of these "nanocomposites" by a variety of methods including sol-gel approaches has been reported. The general objective in synthesizing this type of hybrid material was to incorporate the conducting polymer within the lamellar spaces of the layered inorganic oxides [3-6]. Since the layered V_2O_5 materials are readily prepared by sol-gel approaches, xerogels utilizing V_2O_5 as the inorganic constituent have been investigated and studies of the electrochemical properties of V_2O_5/polyaniline and V_2O_5/polypyrrole xerogels were reported recently [6]. Lithium insertion in these hybrid materials was reversible and enhanced Li^+ diffusion rates in the electrode were observed.

This paper considers the synthesis, microstructure, and electrochemical properties of aerogels of the inorganic/organic system V_2O_5/polypyrrole. The approach taken with aerogels is quite different from that of the xerogel work. With the aerogel materials, the objective is to attain two interpenetrating networks: V_2O_5 to achieve lithium intercalation and polypyrrole (PPy) to provide an electronically conducting network. This approach would circumvent the need to add carbon to electrode structures because of the low electronic conductivity of the transition metal oxide. In addition, the ability of PPy to intercalate lithium should be advantageous for lithium capacity. A key feature in designing this hybrid material is the need to have a homogeneous distribution of the conducting polymer so that good access to the V_2O_5 phase is achieved. Our prior paper on V_2O_5/PPy nanocomposite materials focused primarily on the interaction between the constituent phases and its influence on electrical and electrochemical properties [7]. The present paper considers the microstructural development of these hybrid networks using alternative synthetic routes.

2. EXPERIMENTAL

Composite aerogels of V_2O_5 and PPy were synthesized according to three different sol-gel approaches. The first approach was to synthesize a "microcomposite" consisting of preformed particles of PPy homogeneously dispersed within a matrix of V_2O_5 aerogel. A second approach, "post-gelation polymerization" (PGP), involved consecutive polymerization of the inorganic and organic phases by first allowing the V_2O_5 to gel from its own sol, then introducing the pyrrole monomer and a polymerizing agent. The third approach, termed "cosynthesis", was to polymerize the organic and inorganic networks simultaneously from a common solution. The nature of the interactions between the inorganic and organic constituents are found to be the most important factors in determining the final microstructures.

2.1. Microcomposite Synthesis

V_2O_5 /PPy microcomposite aerogels were synthesized by forming the oxide gel in the presence of a dispersion of preformed PPy. Pyrrole was polymerized and electronically doped according to the procedure used by Myers [8]. Monomer was added dropwise to a 0.4 M solution of ferric chloride in diethyl ether until a pyrrole concentration of 0.1 M was reached. The glass container was maintained at 0 °C by immersion in an ice bath. The monomer was converted immediately after contacting the oxidizing solution, as evidenced by the characteristic black color of PPy. After one hour, the precipitated reaction product was filtered (1.6 μm pore size) and rinsed thoroughly with deionized water, 10 % hydrochloric acid, additional deionized water (until water was pH-neutral), ethanol, and finally diethyl ether. The washed solid was vacuum dried for 4 hours at 65 °C and ground into a fine powder.

The desired quantity of PPy was added to a solution of water and acetone. A relatively stable dispersion was formed by stirring the mixture with an automatic stirrer at 8000 rpm. The polymer dispersion was poured into the casting vial containing vanadyl triisopropoxide (1:40:17 molar ratio of V:water:acetone), shaken quickly, and the mixed sol gelled in several seconds. After at least 4 days of aging in sealed vials, the hybrid gels were washed thoroughly in acetone to remove residual water, unreacted precursor, and isopropanol reaction product. Washed gels were dried by standard supercritical CO_2 extraction in an autoclave resulting in low density, monolithic aerogels.

2.2. Post-Gelation Polymerization

V_2O_5 gels were prepared by a sol-gel synthesis technique developed previously, relying on hydrolysis and condensation of alkoxide precursors [9-11]. A solution of water and acetone was added to one vial, and vanadyl triisopropoxide was added to another. Both vials were cooled in an ice bath prior to mixing. The combined sol was composed of the same 1:40:17 molar ratio of V:water:acetone as discussed above. Gelation occurred within 5-10 seconds, yielding transparent dark red gels which are characteristic of this synthesis route. The wet gels were aged for one week, during which time they turned to an opaque dark green. After aging, the gels were washed thoroughly in acetone to remove residual water, unreacted precursor, and isopropanol reaction product. The gels were then washed in another solvent (methanol, ethanol, acetonitrile, or ethylene glycol) to exchange the acetone for a more suitable polymerization medium for pyrrole. The organic phase was introduced into the inorganic matrix by immersing the washed V_2O_5 gels in a solution of pyrrole monomer (0.15-0.45 M) in the same solvent that was previously exchanged into the V_2O_5 pore structure. The gels were soaked in the monomer solution for at least 24 hours at 25 °C to allow an equilibrium concentration of pyrrole to be established within the pores of the

aged V_2O_5 gel. The pyrrole-impregnated gels were then transferred into an oxidizing solution consisting of either $FeCl_3$ or $Fe(NO_3)_3$ in the chosen polymerization solvent. Oxidizing solutions varied in concentration (0.30-1.8 M) based on the desired strength and on the concentration of monomer solution used. The purpose of the oxidizing treatment was to complete oxidative polymerization of unreacted pyrrole and achieve oxidative doping of PPy. After 24 hours in the oxidizing solution, the hybrid gels were again washed thoroughly in acetone before drying treatments were initiated. The drying of wet gels proceeded either by standard supercritical CO_2 extraction in an autoclave or by the evaporation of pentane from solvent-exchanged gels under ambient conditions [12]. Both drying techniques resulted in low density, monolithic aerogels.

2.3. Cosynthesis Procedure

A solution of vanadyl triisopropoxide and pyrrole in ethanol was mixed into a vial and cooled in an ice bath. An aqueous solution of either $FeCl_3$ or $Fe(NO_3)_3$ (0.02-0.75 M) was prepared in a separate vial and also cooled in an ice bath. The aqueous solution was added to the monomer solution and agitated quickly. This approach promotes molecular level mixing of the precursors and the polymerization initiators of both networks. A typical ratio used in the cosynthesis procedure was 1:1:1:40:17 (V:pyrrole:Fe:water:acetone), although precursor ratios were varied to study the effects of sol interactions on nanocomposite morphology and properties. Each sol turned the characteristic black color of PPy as soon as the oxidizing solution was added, indicating that the organic polymerization reaction begins immediately. The viscosity of the sols increased until gelation occurred. Gelation times varied between 1 second and 3 minutes, depending on the ratio of precursors and the particular oxidizing solution used. The wet gels were aged for one week and then washed thoroughly in acetone. Monolithic aerogels were prepared using the same drying methods as described for PGP gels.

2.4. Characterization Methods

The fraction of porosity in the hybrid aerogels was obtained by comparing the skeletal density determined by He pycnometry (Micromeritics Accupyc 1330) with the bulk density determined by Hg pycnometry. Surface area measurements were carried out using N_2 adsorption (Micromeritics ASAP 2010) on vacuum dried specimens and analyzed by the BET method. TGA measurements (TA Instruments TGA 295) were performed in N_2 and air using a heating rate of 10 °C/min. FTIR spectra from 4800-400 cm^{-1} were recorded from KCl pellets with a Nicolet 510P spectrophotometer. Tian and Zerbi's "effective conjugate coordinate" (ECC) theory explains relations between PPy's vibrational spectrum and properties [13,14]. Structural changes which occur during polymerization of the monomer as well as the approximate doping level of the polymer are correlated with the spectral features. For example, the

intensity ratio of the peaks at around 1560 and 1480 cm^{-1} are inversely proportional to the average conjugation length and the conductivity of the polymer [15]. Electron microscopy was performed using a Cambridge Stereoscan 250SEM for SEM samples and a JEOL model 100CX for TEM samples. TEM specimens were prepared by applying a fine dispersion of sample material in acetone onto a copper grid and allowing the solvent to dry completely.

Electrical conductivity of the resulting materials was determined using two different methods. The conductivity of aerogel disks (1 cm dia. and 1 cm thick) was measured by two point complex impedance (20 Hz - 1 MHz) from 150 °C to 25 °C in flowing argon as described previously [10]. The conductivity of pressed pellets was determined using a commercial four-point probe (Magne-tron Instruments M-700) with a tip spacing of 0.1 cm. For this measurement, powders were compressed at 1 GPa pressure applied for 60 seconds to produce samples of approximately 0.1 cm thickness by 1.3 cm diameter. The conductivity (d.c.) was obtained only at room temperature and represents a screening method to determine the effect of synthesis conditions on nanocomposite conductivity.

Cyclic-voltammetry (CV) was used to compare the electrochemical properties of the various V_2O_5/PPy hybrid materials with those of pure V_2O_5 aerogels. Three electrode cells were constructed with Li metal as counter and reference electrodes and a 1 M solution of $LiClO_4$ in propylene carbonate as the electrolyte. The working electrode was a composite film composed of active material, Ketjenblack carbon, and polyvinylidene fluoride (PVDF) binder with a weight ratio of 80:20:5, respectively. The composite films were prepared by stirring the component powders in n-methyl-2-pyrrolidinone (NMP) for at least 3 days before spreading the paste into a thin film on a stainless steel current collector. The composite electrodes were dried under vacuum at 125 °C for 18 hours to remove free water and residual NMP prior to assembling the electrochemical cell in an Ar filled glovebox. Working electrodes had a surface area of about 4 cm^2 and contained between 0.6-1.6 mg of active material. Electrochemical data were acquired by a PC-controlled potentiostat (EG & G Princeton Applied Research model 273A). Voltage cycles were made with a sweep rate of 0.1 mV/sec between the initial open circuit value (about 3.6 V vs. Li) and 1.8 V vs. Li.

3. RESULTS AND DISCUSSION

3.1. Microcomposites

The microcomposite synthesis approach resulted in a uniform dispersion of micron and submicron sized PPy particles encapsulated in a matrix of V_2O_5 aerogel (Figure 1), indicating that the organic particles did not settle significantly prior to gelation of the inorganic network. The FTIR spectrum of the resulting material (Figure 2) indicates the presence of each phase without any evidence of interaction between them

(i.e. no peak shifts relative to the PPy and V_2O_5 reference spectra). Table 1 shows that the microcomposite materials are highly porous but that they become more dense and have reduced surface as a result of the addition of PPy.

Although the PPy phase was determined to have a high conductivity prior to mixing (d.c. conductivity of 30 S/cm for pressed pellet), the particles are too isolated to form a conductive pathway through the aerogel material. If the conductivity of an insulating phase is to be increased by the addition of conductive particles, a minimum volume fraction of the conducting phase must be reached. There are several percolation theory models applied to various mixture configurations [16,17]. Kirkpatrick and Zallen's model predicts a percolation threshold of 16 % by volume for three-dimensional, random packing of spherical particles. To illustrate the problem of obtaining percolation of a dense PPy phase (1.6 g/cm^3) throughout a V_2O_5 aerogel phase (0.07 g/cm^3), a composition of $[PPy]_{14}V_2O_5$ would be required to achieve 16 % pyrrole by volume. The data in Table 1 suggest how such an excess of PPy would adversely affect the high surface area morphology of the aerogel. Additionally, the primary electrochemically active phase, V_2O_5, would be diluted to 19 % by mass at this composition. Thus, the limitation of the microcomposite approach is that achieving a conductive electrode is expected to result in low specific capacity. A more effective route is to design nanocomposite materials which do not require as much PPy in order to bring electrons locally to V_2O_5 intercalation sites. Fournier *et al.* reported percolation thresholds of around 15 % by volume for composites of carbon in an epoxy matrix, and less than 3.5 % by volume for composites of PPy in epoxy [18]. This dramatic difference was attributed to the fractal-like morphology of the PPy network in contrast to the non-fractal clusters of carbon black. It is expected that a similarly fractal-like network of PPy distributed homogeneously throughout a porous matrix should reduce the percolation threshold far below the 16 % required for the microcomposites. The post-gelation polymerization and cosynthesis strategies are focused in this direction.

3.2. Post-Gelation Polymerization

The PGP experiments explored different chemical polymerization approaches for PPy. Methanol, ethanol, and acetonitrile were used as polymerization media with $FeCl_3$ as the oxidizing agent. Methanol was eliminated as a candidate, as it caused dissolution of the V_2O_5 network structure during the first washing cycles of the preformed gels. The V_2O_5 gels remained intact in the washing and pyrrole impregnation steps when ethanol and acetonitrile were used. After soaking these hybrid gels in $FeCl_3$ solutions and washing them several times in acetone, they were supercritically dried. The physical properties of monolithic aerogels from the PGP method are tabulated in Table 2. TEM studies of these materials (Figure 3) revealed aggregations of PPy supported by ribbon-like structures which are characteristic of V_2O_5 gel networks [19]. Moreover, there is an indication that the V_2O_5 matrix is unstable in $FeCl_3$ solutions. The skeletal density of the aerogels was much lower than that expected from the

starting ratio of V_2O_5:PPy (i.e. due to higher PPy content) and their FTIR spectra (Figure 4) exhibit very small peaks, if any, from the V_2O_5 phase. The similarity between the spectra from the PGP hybrid materials (figure 4b and c) and the PPy (figure 4a) confirms that the hybrid is primarily composed of the organic constituent. The d.c. conductivity values for pressed pellets of these materials (2-7 x 10^{-3} S/cm) were between those of V_2O_5 aerogel (< 10^{-5} S/cm) and pure PPy synthesized in $FeCl_3$/acetonitrile (5.6 x 10^{-2} S/cm).

The influence of two different oxidizing solutions, $FeCl_3$ and $Fe(NO_3)_3$ in ethanol, was compared by soaking V_2O_5 gels in either medium for 6 hours. The oxidation treatment was followed by washing in acetone and then pentane before drying under ambient conditions. The resulting aerogels exhibited an obvious difference in appearance. The $FeCl_3$ treated gels were discolored brown with a distorted shape whereas the $Fe(NO_3)_3$ treated gels exhibited much the same appearance as untreated V_2O_5 aerogels (dark green cylinders). Although the $FeCl_3$ solution is intended only to polymerize and dope the organic phase, these results indicate that it also has adverse effects on the V_2O_5 gel structure. In contrast, $Fe(NO_3)_3$ oxidizing solutions appear to be relatively inert with respect to the inorganic gel.

Ethanol, acetone, and ethylene glycol were used as polymerization media for $Fe(NO_3)_3$ oxidized PGP materials. The V_2O_5 gel structure was stable in each of these solvents during washing and pyrrole impregnation steps. After oxidation, the hybrid gels were dried from supercritical CO_2 or ambient pentane. Both methods yielded rigid monolithic materials, the properties of which are given in Table 2. Supercritically dried aerogels exhibited porosity fractions between 90-96 %. Skeletal density values were between 2.1-3.3 g/cm^3, corresponding to a composition range of 0.5-4.5 PPy/V_2O_5. TEM micrographs (Figure 3b) revealed an inhomogeneous microstructure similar to the PGP samples oxidized in $FeCl_3$ solutions. The measured d.c. conductivities of pressed pellets were all below 10^{-5} S/cm.

Cyclic voltammetry was carried out on the PGP hybrid material oxidized in $Fe(NO_3)_3$/ethylene glycol solution and dried from ambient pentane. The composition was determined to be $[PPy_{3.5}]V_2O_5$ from TGA data (Figure 5). The CV data (Figure 6) exhibit intercalation and deintercalation peaks from the V_2O_5 phase at 2.6 and 2.8 V vs. Li, respectively, as seen in the CV data for the pure V_2O_5 aerogel reference (included in Figure 6). Additional intercalation capacity at around 2.2 V vs. Li was observed in the presence of the PPy phase. The amount of reversible lithium intercalation capacity of the PGP hybrid material was 1.4 Li per $[PPy]_{3.5}V_2O_5$. The specific capacity of this electrode, 95 mAh/g, is less than half of that for an electrode prepared with pure V_2O_5 aerogel (dried from ambient pentane) and cycled under comparable conditions [7,11]. The electronic and electrochemical activity of the PPy phase in PGP hybrid materials appears to be insignificant compared to its mass contribution in this material.

The PGP approach brings considerable improvements over the microcomposite materials in that true nanocomposites are formed. Nanometer scale mixing of the V_2O_5 and PPy phases is important in reducing the amount of PPy required to achieve a percolation of conductive pathways through the gel, however, a homogeneous distribution of the conductive phase is also beneficial. Unfortunately, the

microstructure of PGP derived materials consists of aggregates of PPy isolated from one another in the V_2O_5 network (Figure 3). Another limitation of the PGP method is that compositional control is difficult because it depends on the concentrations of pyrrole and oxidizing agent which diffuse into the pore volume of the gel. If conductive pathways are to be introduced with a minimum amount of PPy added to the microstructure, a synthetic approach must be developed which produces uniform materials with controlled compositions. The cosynthesis approach addresses these considerations.

3.3. Cosynthesis Gels

The cosynthesis method has several adjustable parameters which offer an opportunity to tailor the properties and morphology of the hybrid material. The most important parameters are (1) the temperature of the polymerization reactions; (2) the selection of cosolvent and oxidizing agent; and (3) the relative concentrations of precursors. Several combinations of these parameters were explored in order to determine their respective influences, as well as to determine the nature of the interactions occurring in the precursor solution.

The initial reaction temperature for these experiments was fixed at 0 °C to slow the rapid polymerization kinetics of the inorganic and organic phases. This condition was also selected because prior work has shown that in the chemical synthesis of PPy, decreasing the reaction temperature correlated with increasing conductivity of the product, especially over the temperature range 0-20 °C [20].

The studies directed at finding an effective cosolvent/oxidizer combination considered a number of effects including PPy conductivity and stability of the V_2O_5 network. Acetone is a logical cosolvent candidate because of its use in the gelation of vanadyl alkoxides [9-11]. However, acetone is not the best choice of solvent from which to polymerize conductive PPy. The conductivity of chemically synthesized PPy has also been shown to be a function of the oxidation potential of the polymerization medium [20]. In this respect, acetone was shown to perform significantly worse than that of other solvents such as methanol, ethanol, ethylene glycol, or water. These conclusions are consistent with our 4-probe conductivity measurements of pressed pellets of chemically synthesized PPy. Table 3 shows that the conductivity of PPy varies over several orders of magnitude depending on the combination of solvent and oxidizing agent used in the synthesis. In general, there is good agreement between measured conductivity values in Table 3 and those reported in the literature [8,21,22].

In the investigation of different alcohols, methanol was eliminated because it tends to dissolve the V_2O_5 gel structure. Ethanol was considered because it was reported to be an effective solvent in the hydrolysis and condensation of vanadyl alkoxides [23,24]. To confirm this result, V_2O_5 gels synthesized with ethanol as the solvent were found to produce intact monolithic aerogels. The three vibrational modes characteristic to V_2O_5 gels (V=O, V-O-V_{asym}, and V-O-V_{sym} stretches) were present in the FTIR data (Figure 7a,b), although the vanadyl stretch ($\upsilon_{V=O}$) occurred at a slightly red-shifted frequency (994 cm^{-1})

relative to the same vibration in V_2O_5 gels derived from acetone/water sols (1001 cm^{-1}). Ethylene glycol was also evaluated as a solvent for the gelation of V_2O_5. The resulting gels exhibited similar gelation times and physical characteristics as those using ethanol as the solvent.

The selection of the oxidizing agent was based on its effect on V_2O_5 gelation. Upon adding various oxidizing agents $(FeNO_3)_3$, $FeCl_3$, ferric sulfate, ferric ammonium sulfate, and potassium ferrocyanide) at 1 M concentrations to the typical vanadium oxide sol, only the $Fe(NO_3)_3$ containing sample became a V_2O_5 xerogel with the expected FTIR spectrum (Figure 7c). The other samples exhibited precipitation. The reason for this behavior is that V^{4+} centers act as polymerization initiators for the formation of V_2O_5 gel ribbons [19]. An oxidizing agent that dramatically increases the amount of V^{5+} with respect to V^{4+} will thus inhibit V_2O_5 gel formation.

A series of hybrid aerogels was prepared with pyrrole/V ratios ranging from 0.3 to 1.0 utilizing the above mentioned synthesis parameters of 0 °C reaction temperature and ethanol (or ethylene glycol) as the solvent. The effect of $Fe(NO_3)_3$ concentration on the morphology, composition, and properties of these aerogels was investigated in detail and is discussed below. Typical physical properties of these hybrid aerogels are shown in Table 2. These cosynthesis materials exhibit the usual aerogel morphology of low density (0.1-0.2 g/cm^3) and high surface area (200-300 m^2/g). The pore size distribution of a cosynthesis aerogel shows a high specific volume occupied by pores in the 100 to 1000 Å size range (e.g. 1.2 cm^3/g), in contrast with the lower and relatively uniform distribution of pore volumes in the V_2O_5 aerogel (Figure 8). The presence of more large pores in the hybrid aerogel is consistent with the calculated average pore size data. The hybrid aerogel material exhibits an average pore size of 160 Å, while that of the V_2O_5 aerogel sample is only 80 Å. The presence of fully or partially polymerized pyrrole in the sol is likely to physically block the growth of V_2O_5 ribbons. The disruption of the gel network may account for the increase in the presence of larger pores.

For a given pyrrole:vanadyl alkoxide ratio (0.5 Py/V), the change in concentration of $Fe(NO_3)_3$ in the sol (from 0.0-2.0 Fe/V) had a large effect on the composition of the gel. This behavior is evident from the FTIR spectra (Figure 9), TEM micrographs (Figure 10), and is verified by the TGA data (not shown). Below 0.05 Fe/V, the PPy content of the dried gels was lower than expected, based on the nominal composition of the sol. As the V_2O_5 network begins to form, it provides initiation sites for the oxidative polymerization of nearby pyrrole monomer. The ability of oxide surfaces to initiate oxidative polymerization of pyrrole has been demonstrated for manganese oxide [25,26] and silica [27]. However, the oxide network is apparently unable to cause complete conversion of the organic monomer, and the unreacted monomer is washed away during the solvent exchange step.

The interaction between the pyrrole monomer and the vanadyl alkoxide is evident from two features: the nature of the morphology of the V_2O_5 phase and the composition of the final hybrid aerogel. TEM micrographs (Figure 10) show the microstructural differences between V_2O_5 and cosynthesis hybrid aerogels. The characteristic ribbon structures of the V_2O_5 aerogel are much shorter when the sol contains

pyrrole. This morphology change is attributed to the redox reactions between the precursors in which V^{5+} centers are reduced to V^{4+} from the oxidation of pyrrole. With more V^{4+} to initiate V_2O_5 ribbon growth, it is not surprising that the average length of V_2O_5 ribbons in the gel structure is shorter. It is important to note that the distribution of the PPy phase is much more homogeneous in the cosynthesis hybrids than in the PGP hybrid materials (Figure 3).

The concentration of oxidizing agent added in the synthesis has a significant effect on composition of the final aerogel hybrid. A series of samples was prepared in which the pyrrole:vanadyl alkoxide ratio was 0.5 and the concentration of $Fe(NO_3)_3$ added to the sol varied from 0 to 2.0 Fe/V. Below 0.05 Fe/V, the PPy content for the final aerogel was lower than 0.5 pyrrole/V of the initial composition. It would seem that pyrrole is removed during the washing step because the oxide network is unable to achieve complete oxidative polymerization of the monomer. Upon increasing the $Fe(NO_3)_3$ concentration above 0.05 Fe/V, the PPy content of the final aerogel becomes progressively higher than 0.5 [PPy]/V. There are two contributing factors to this composition variation: there is now adequate oxidative polymerization of pyrrole within the sol; and the increasing amount of V^{5+} (with respect to V^{4+}) caused by adding the oxidizing agent inhibits gel formation. It is now the vanadyl alkoxide which is removed during the washing step. At 0.05 Fe/V, the composition of the aerogel matches the 0.5 [PPy]/V composition ratio of the precursors. Unfortunately, this amount of oxidizing agent does not dope the PPy adequately.

These results indicate the difficulty in achieving a highly conductive PPy phase. The V_2O_5 network itself is unable to provide sufficient initiation sites for oxidative polymerization of the organic monomer, thus requiring the addition of $Fe(NO_3)_3$ as an oxidizing agent. If too little is added to the sol, the PPy is not doped sufficiently to obtain the high conductivity state and the conductivity of the hybrid aerogel is comparable to that of the V_2O_5 matrix. If a high concentration of $Fe(NO_3)_3$ is added, the lack of V^{4+} inhibits gelation of the V_2O_5 phase. For example, a sol containing 1.0 pyrrole/V and a large excess of $Fe(NO_3)_3$ (2.0 Fe/V) resulted in a hybrid aerogel with a composition of $[PPy]_{8.5}V_2O_5$. The V_2O_5 network of this sample consists of very short ribbons or platelets coated with a layer of PPy (Figure 10d). Pressed pellet measurements indicated that the material is at least 100 times more conductive than V_2O_5, however, there is too little volume fraction of V_2O_5 remaining in the hybrid for it to be utilized as a reversible lithium electrode.

The lithium intercalation properties of the co-synthesized hybrid aerogels are strongly influenced by the concentration of oxidizing agent in the sol which, in turn, affects the hybrid composition as discussed above. Thus the specific capacity is lowest for the hybrid material prepared using the largest amount of $Fe(NO_3)_3$ because the resulting composition is greatly increased in PPy content (Table 4). Although this hybrid possesses a higher electronic conductivity as compared to V_2O_5, its specific capacity for lithium is reduced because the intercalation properties of PPy are substantially poorer than V_2O_5. The CV data (Figure 11) exhibit only broad intercalation and deintercalation peaks centered at 2.5 and 2.9 V vs. Li, respectively, which are characteristic of PPy [28-30]. By limiting the $Fe(NO_3)_3$ concentration to

0.05 Fe/V, the lithium capacity of the resulting hybrid improves significantly and values within 10 % of that exhibited by V_2O_5 aerogels are achieved. The CV data (Figure 12) show intercalation and deintercalation peaks from the V_2O_5 phase at 2.6 and 2.8 V vs. Li, respectively. The lithium capacity for aerogel hybrids without any oxidizing agent were virtually the same as that of V_2O_5 aerogels.

If the PPy phase is to contribute a high electronic conductivity to the hybrid electrode without significantly reducing the specific capacity, at least two conditions must be met. First, it must be uniformly distributed such that the concentration at which percolation occurs is kept to a minimum relative to the V_2O_5 phase. Second, it must be polymerized in a suitable medium and be sufficiently doped such that the highly conductive form of the polymer is obtained. The cosynthesis approach with no oxidizing agent satisfies the requirements that both phases are distributed homogeneously and that the polymerization medium can promote the formation of conductive PPy. A suitable doping procedure remains to be found.

4. CONCLUSIONS

Vanadium pentoxide/polypyrrole hybrid monolithic aerogels have been prepared using three different strategies and under varied synthesis conditions. Unique microstructures are formed by each of the synthesis approaches, resulting primarily from the network formation sequence of the two constituent phases. Microcomposite materials were formed by precipitating conductive PPy from a solution of pyrrole monomer and then gelling the V_2O_5 phase around this preformed polymer. The materials from this group were comprised of a lithium intercalating V_2O_5 aerogel matrix supporting a dispersion of high conductivity PPy particles. The post-gelation polymerization approach also involves sequential polymerization of the component networks. In this case, the oxide gel is preformed and impregnated with the organic monomer which is then polymerized and doped using an oxidizing solution. However, the organic polymer in the resulting gels is distributed inhomogeneously throughout the oxide gel network and forms aggregates instead of a continuous conductive network. The cosynthesis approach, where inorganic and organic precursors are allowed to polymerize concurrently, results in a homogeneous distribution of the PPy and the V_2O_5 phases. The designed microstructure and composition have been obtained through this route, although a suitable doping procedure is still required in order to oxidize PPy into its high conductivity state. Interactions between the oxidizing agent and the oxide phase were deleterious to the structure and composition of the gel. The electrochemical properties of each of these hybrid materials show that the [PPy]/V_2O_5 ratio is critical in obtaining electrode materials with high specific capacity.

ACKNOWLEDGMENTS

The authors greatly appreciate the financial support of this work by the Office of Naval Research (BD) and the Natural Sciences and Engineering Council of Canada (LFN). Also acknowledged is helpful advice from F. Leroux regarding experimental considerations and TEM from Wei Cheng.

REFERENCES

1. C. Sanchez and F. Ribot, *New J. Chem.*, **18** (1994), pp. 1007-1047.
2. P. Judeinstein and C. Sanchez, *J. Mater. Chem.*, **6** (1996), pp. 511-525.
3. M.G. Kanatzidis, C.-G. Wu, H.O. Marcy, D.C. DeGroot, and C.R. Kannewurf, *Chem. Mater.*, **2** (1990), pp. 222-224.
4. L. Wang, J. Schindler, J.A. Thomas, C.R. Kannewurf, and M.G. Kanatzidis, *Chem. Mater.*, **7** (1995), pp. 1753-1755.
5. G.-C. Wu, D.C. DeGroot, H.O. Marcy, J.L. Schindler, C.R. Kannewurf, Y.-J. Lui, W. Hirpo, and M.G. Kanatzidis, *Chem. Mater*, **8** (1996), pp. 1992-2004.
6. F. Leroux, G. Goward, W.P. Power, and L. Nazar, *J. Electrochem. Soc.*, **144** (1997), pp. 3886-3895.
7. H.P. Wong, B.C. Dave, F. Leroux, J. Harreld, and L.F. Nazar, *J. Mater. Chem.*, **8** (1998), pp. 1019-1027.
8. R.E. Myers, *J. Electronic Mater.*, **15** (1986), pp. 61-69.
9. B. Katz, W. Lui, K. Salloux, F. Chaput, B. Dunn, and G.C. Farrington, *Mater. Res. Soc. Symp. Proc.*, **369**, (1992), pp. 211-222.
10. F. Chaput, B. Dunn, P. Fuqua, and K. Salloux, *J. Non-Cryst. Solids*, **188** (1995), pp. 11-18.
11. H.P. Wong, B. Dunn, K. Salloux, F. Chaput, and M.W. Breiter, *Electrochem. Soc. Symp. Proc.*, **95-22** (1996), pp. 46-52.
12. J.H. Harreld, W. Dong, and B. Dunn, *Mat. Res. Bull.*, **33** (1998), pp. 561-567.
13. B. Tian and G. Zerbi, *J. Chem. Phys.*, **92** (1990), pp. 3886-3891.
14. B. Tian and G. Zerbi, *J. Chem. Phys.*, **92** (1990), pp. 3892-3898.
15. J. Wei, W. Liang, and C.R. Martin, *Synth. Met.*, **48** (1992), pp. 301-312.
16. D.S. McLachlan, M. Blaszkiewicz, and R.E. Newnham, *J. Am. Ceram. Soc.*, **73** (1990), pp. 2187-2203.
17. F. Lux, *J. Mater. Sci.*, **28** (1993), pp. 285-301.
18. J. Fournier, G. Boiteux, G. Seytre, and G. Marichy, *Synth. Met.*, **84** (1997), pp. 839-840.
19. J. Livage, *Chem. Mater.*, **3** (1991), pp. 578-593.

20. S. Machida, S. Miyata, and A. Techagumpuch, *Synth. Met.*, **31** (1989), pp. 311-318.
21. E. Dalas, S. Sakkopoulos, and E. Vitoratos, *J. Mater. Sci.*, **29** (1994), pp. 4131-4133.
22. J.C. Thiéblemont, J.L. Gabelle, and M.F. Planche, *Synth. Met.*, **66** (1994), pp. 243-247.
23. H. Hirashima, K. Tsukimi, and R. Murataki, *J. Ceram. Soc. Jap., Intl. Ed.*, **97** (1989), pp. 232-235.
24. H. Hirashima and K. Sudoh, *J. Non-Cryst. Solids*, **145** (1992), pp. 51-54.
25. S. Kuwabata and H. Yoneyama, *Mater. Res. Soc. Symp. Proc.*, **393**, (1995), pp. 125-130.
26. A.H. Gemeay, H. Nishiyama, S. Kuwabata, and H. Yoneyama, *J. Electrochem. Soc.*, **142** (1995), pp. 4190-4195.
27. S. Maeda and S.P. Armes, *J. Mater. Chem.*, **4** (1994) pp. 935-942
28. P. Novák and W. Vielstich, *J. Electrochem. Soc.*, **137** (1990), pp. 1036-1042.
29. P. Novák and W. Vielstich, *J. Electrochem. Soc.*, **137** (1990), pp. 1681-1689.
30. J.Y. Lee, D.Y. Kim, and C.Y. Kim, *Synth. Met.*, **74** (1995), pp. 103-106.

Table 1. Effects of PPy addition on the morphology of microcomposite aerogels (* not measured).

Composition	Density (g/cm^3)	Porosity (%)	Surface area (m^2/g)
V_2O_5	0.1	97	470
$[PPy]_{1.0}V_2O_5$	0.1	96	*
$[PPy]_{2.0}V_2O_5$	0.2	92	140
$[PPy]_{6.0}V_2O_5$	0.2	89	80

Table 2. Physical properties of hybrid aerogels derived from PGP and cosynthesis methods (* not measured).

Synthesis Method	Nominal Composition (Py/V)	Drying Conditions	Surface Area (m^2/g)	Porosity (%)
PGP (acetone/$Fe(NO_3)_3$)	0.33	supercritical	340	95
PGP (acetone/$Fe(NO_3)_3$)	1.0	supercritical	270	90
PGP (acetone/$FeCl_3$)	1.0	supercritical	*	93
PGP ($CH_3CN/FeCl_3$)	1.0	supercritical	*	94
Cosynthesis (acetone/$Fe(NO_3)_3$)	0.33	supercritical	190	97
Cosynthesis (ethanol/$Fe(NO_3)_3$)	0.5	supercritical	290	97
Cosynthesis (EG/$Fe(NO_3)_3$)	0.5	ambient	190	*
Cosynthesis (ethanol/$Fe(NO_3)_3$)	1.0	ambient	*	88

Table 3. Percent yield (based on a 2 g charge of pyrrole monomer) and d.c. conductivity of chemically polymerized PPy from various oxidizing solutions (* not measured). T = O °C, [pyrrole] = 0.14 M, and [oxidizing agent] = 0.56 M.

Oxidizing solution	Yield (%)	Conductivity (S/cm)
acetone/water/$Fe(NO_3)_3$	108	$< 10^{-3}$
CH_3CN/water/$Fe(NO_3)_3$	57	0.003
n-propanol/water/$Fe(NO_3)_3$	63	0.07
ethanol/water/$Fe(NO_3)_3$	*	0.10
EG/water/$Fe(NO_3)_3$	*	0.15
water/$Fe(NO_3)_3$	84	1.0
water/$FeCl_3$	58	4.5
ethanol/water/$FeCl_3$	7	*
EG/water/$FeCl_3$	39	7.5
diethyl ether/$FeCl_3$	97	30

Table 4. Electrochemical results from cosynthesis gels oxidized using $Fe(NO_3)_3$ in ethanol.

Sol Composition		Gel Composition		
Py/V	Fe/V	(from TGA analysis)	Li/V_2O_5	mAh/g
1	0	$PPy_{0.8}V_2O_5$	3.0	240
1	0.05	$PPy_{0.8}V_2O_5$	2.8	180
1	2	$PPy_{8.5}V_2O_5$	1.8	25

Figure Captions

Fig 1. SEM micrographs of (a) highly conductive polypyrrole particles synthesized using a solution of $FeCl_3$ in diethyl ether and (b) a microcomposite hybrid aerogel with a composition of $[PPy]_{2.0}\ V_2O_5$.

Fig 2. FTIR spectra of (a) microcomposite hybrid aerogel with a composition of $[PPy]_{6.0}V_2O_5$ and reference spectra of (b) V_2O_5 and (c) PPy. Peaks from PPy are labeled with designations based on the effective conjugation coordinate (ECC) theory [13,14].

Fig 3. TEM micrographs of PGP hybrid aerogels from (a) $FeCl_3$/ethanol and (b) $Fe(NO_3)_3$/acetone treatments.

Fig 4. FTIR spectra of (a) polypyrrole synthesized in $FeCl_3$/ethanol solution, and PGP hybrids oxidized with (b) $FeCl_3$/ethanol and (c) $FeCl_3/CH_3CN$. The low intensity of peaks from V_2O_5 around 1000 and 760-780 cm^{-1} in (b) or (c) indicates that the hybrid materials are primarily PPy.

Fig 5. TGA data from a hybrid aerogel synthesized by the PGP process using ethylene glycol and $Fe(NO_3)_3$. The initial composition was determined to be $[PPy]_{3.5}V_2O_5 \cdot 1.8H_2O$.

Fig 6. CV scan of (a) $[PPy]_{3.5}V_2O_5$ hybrid aerogel from post-gelation polymerization synthesis and (b) V_2O_5 aerogel reference.

Fig 7. FTIR spectra of V_2O_5 aerogel synthesized with different cosolvents; (a) water/ethanol sol and (b) water/acetone sol. The effect of adding 1M $Fe(NO_3)_3$ oxidizing agent to (b) is shown in (c). The presence of the peaks characteristic of the V_2O_5 phase in spectrum (c) indicates that the V_2O_5 structure is still formed in the presence of $Fe(NO_3)_3$.

Fig 8. Pore size distribution data for (a) cosynthesis aerogel from an ethanol sol containing 0.5 Py/V and (b) V_2O_5 aerogel. The hybrid aerogel contains a much higher specific volume of pores at larger pore sizes (100-1000 Å).

Fig 9. FTIR spectra showing the effect of $Fe(NO_3)_3$ on the gel structure of PPy/V_2O_5 aerogels prepared using the same precursor ratio (0.5 Py/V) and: (a) 0.00 Fe/V; (b) 0.05 Fe/V; and (c) 0.5 Fe/V. Reference spectra for PPy and V_2O_5 aerogel (from H_2O/EtOH sol) are (d) and (e), respectively. It is apparent that the ratio of $[PPy]/V_2O_5$ increases progressively with the addition of $Fe(NO_3)_3$ to the sol.

Fig 10. TEM micrographs of (a) V_2O_5 aerogel synthesized from water/acetone sol and cosynthesis hybrid aerogels prepared with the same precursor ratio (1.0 Py/V) and varying concentrations of $Fe(NO_3)_3$: (b) 0.0; (c) 0.05; and (d) 2.0 Fe/V. The concentration of (c) matches that of the initial sol composition, while (d) leads to a high concentration of PPy.

Fig 11. CV scan of a cosynthesis derived aerogel with a composition of $[PPy]_{8.5}V_2O_5$.

Fig 12. CV scans of cosynthesis $[PPy]/V_2O_5$ aerogel prepared with (a) 0.0 and (b) 0.05 $Fe(NO_3)_3$/vanadyl alkoxide. The reference data from V_2O_5 is shown as (c).

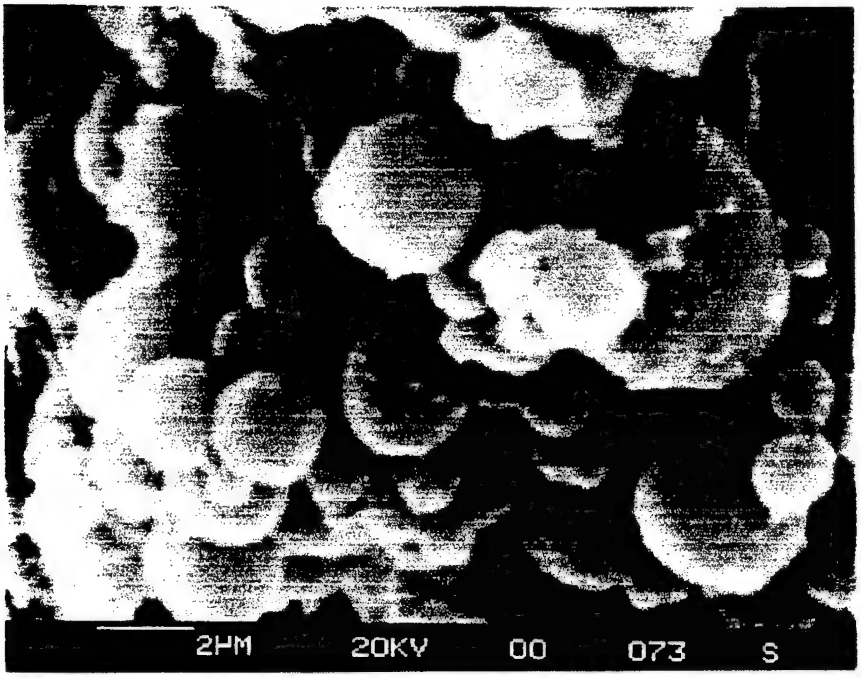

(a)

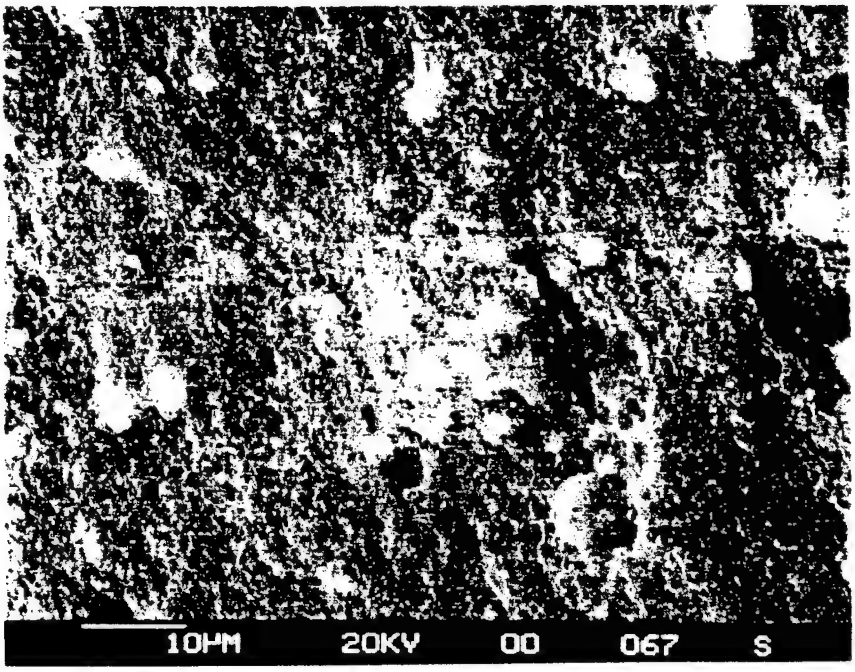

(b)

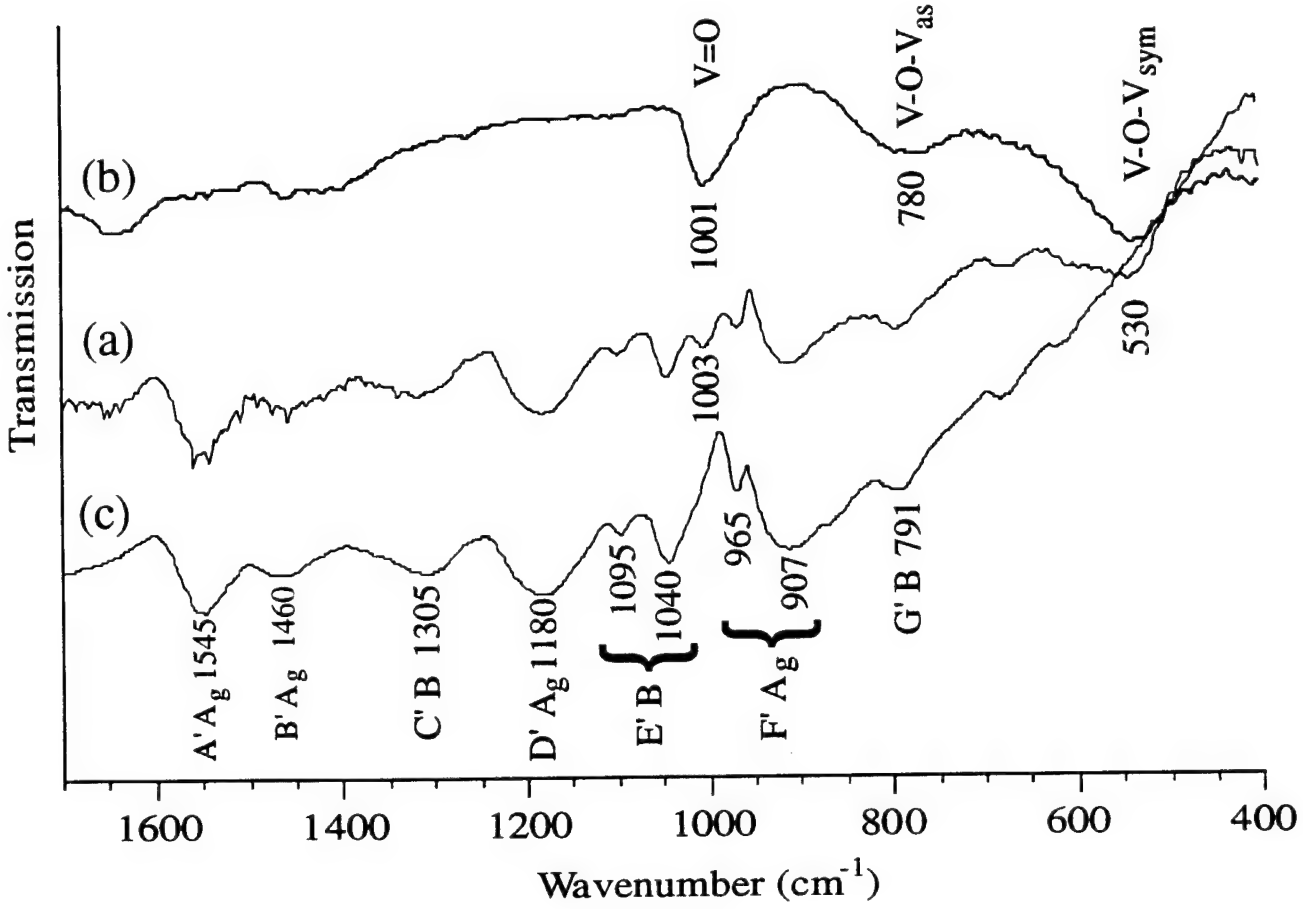
Transmission
(b)
(a)
(c)
V=O
1001
V-O-V as
780
V-O-V sym
530
1003
A' Ag 1545
B' Ag 1460
C' B 1305
D' Ag 1180
E' B
1095
1040
F' Ag
965
907
G' B 791
1600
1400
1200
1000
800
600
400
Wavenumber (cm-1)

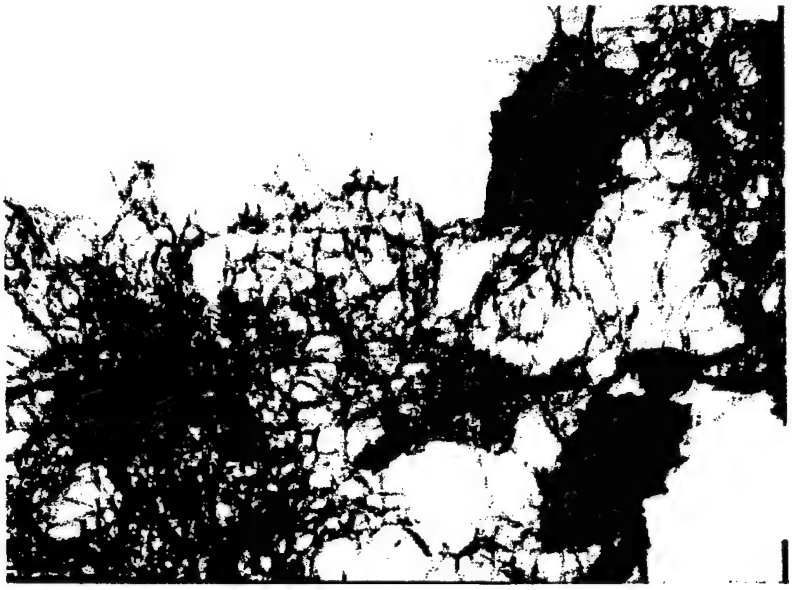

(a) 150 nm

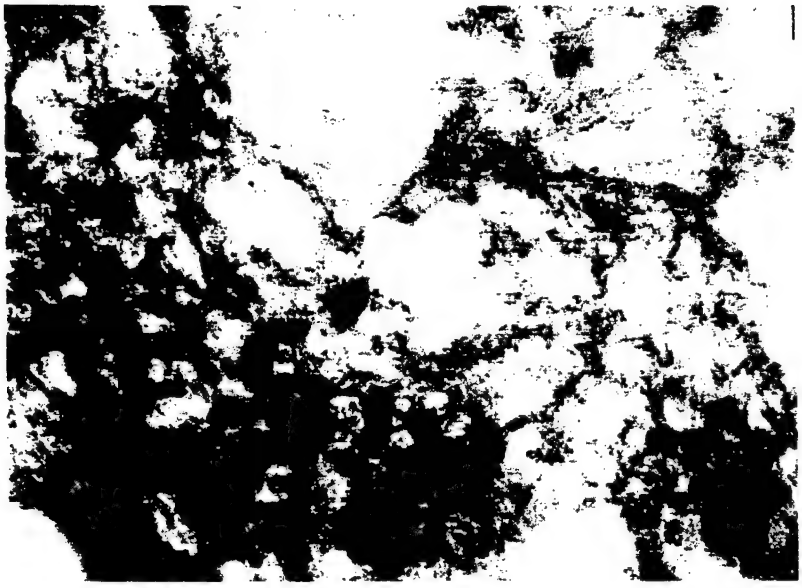

(b) 100 nm

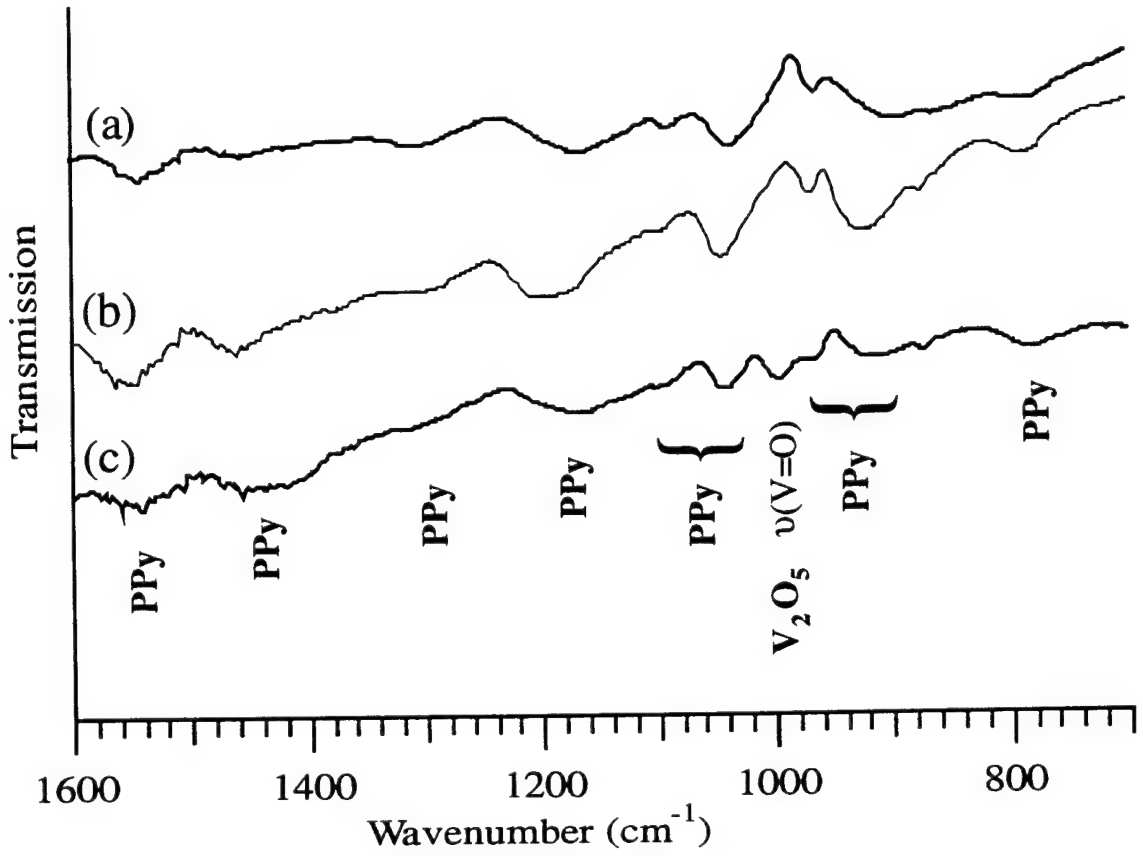
(a)
(b)
(c)
Transmission
PPy
PPy
PPy
PPy
PPy
υ(V=O)
V2O5
PPy
PPy
1600
1400
1200
1000
800
Wavenumber (cm-1)

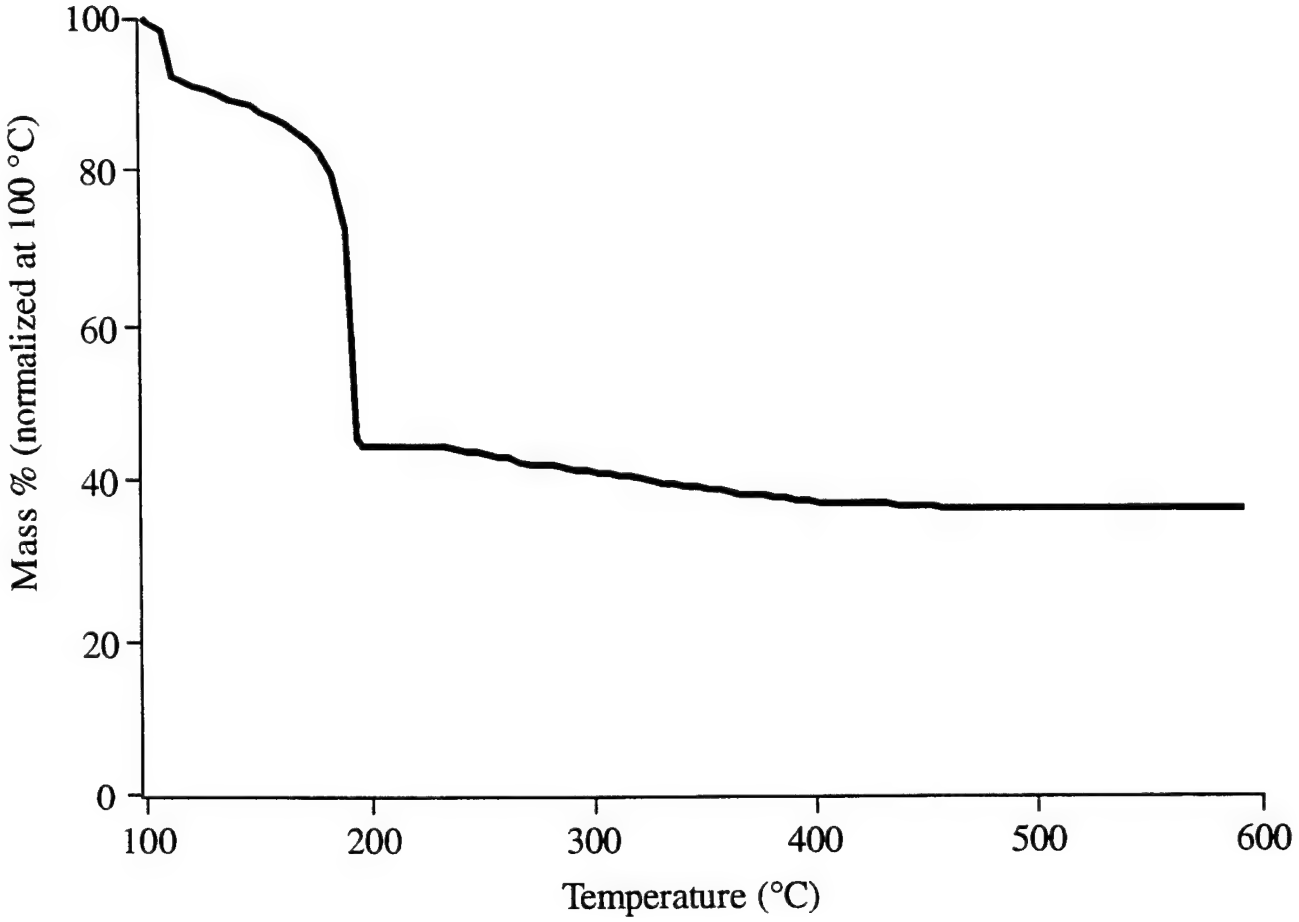
100
80
60
40
20
0
Mass % (normalized at 100 °C)
100
200
300
400
500
600
Temperature (°C)

(a)

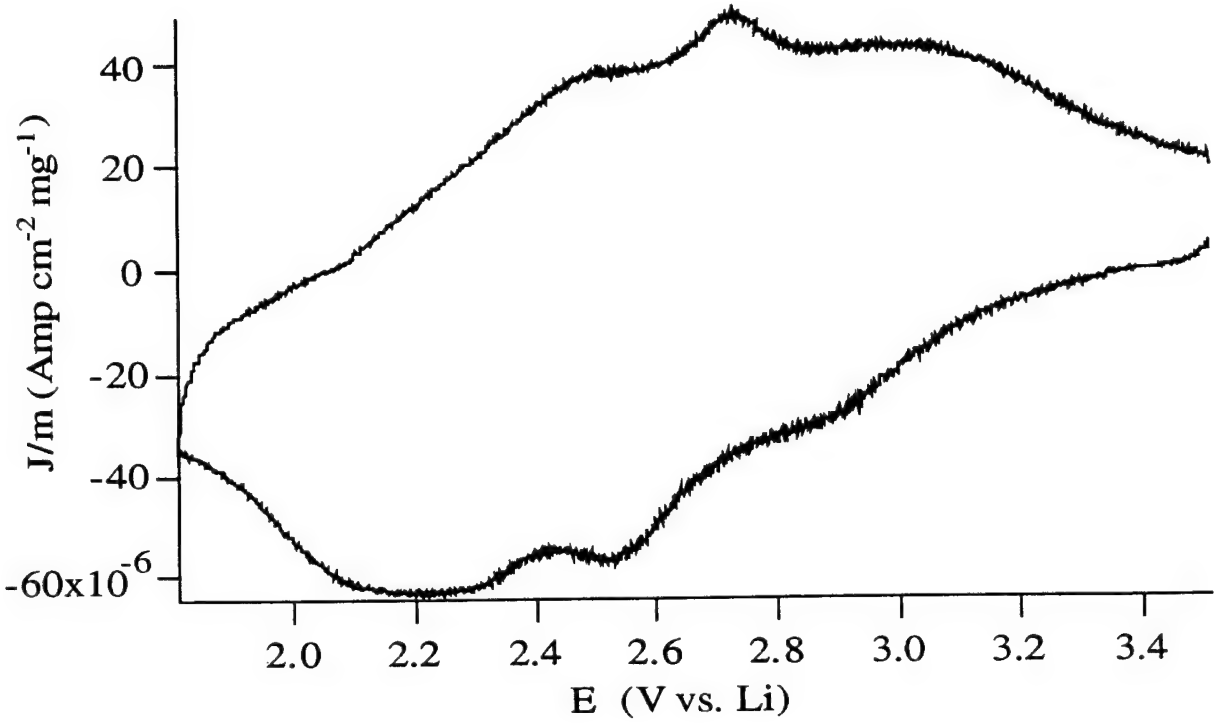
40
20
0
-20
-40
-60x10^-6
J/m (Amp cm^-2 mg^-1)
2.0
2.2
2.4
2.6
2.8
3.0
3.2
3.4
E (V vs. Li)

(b)

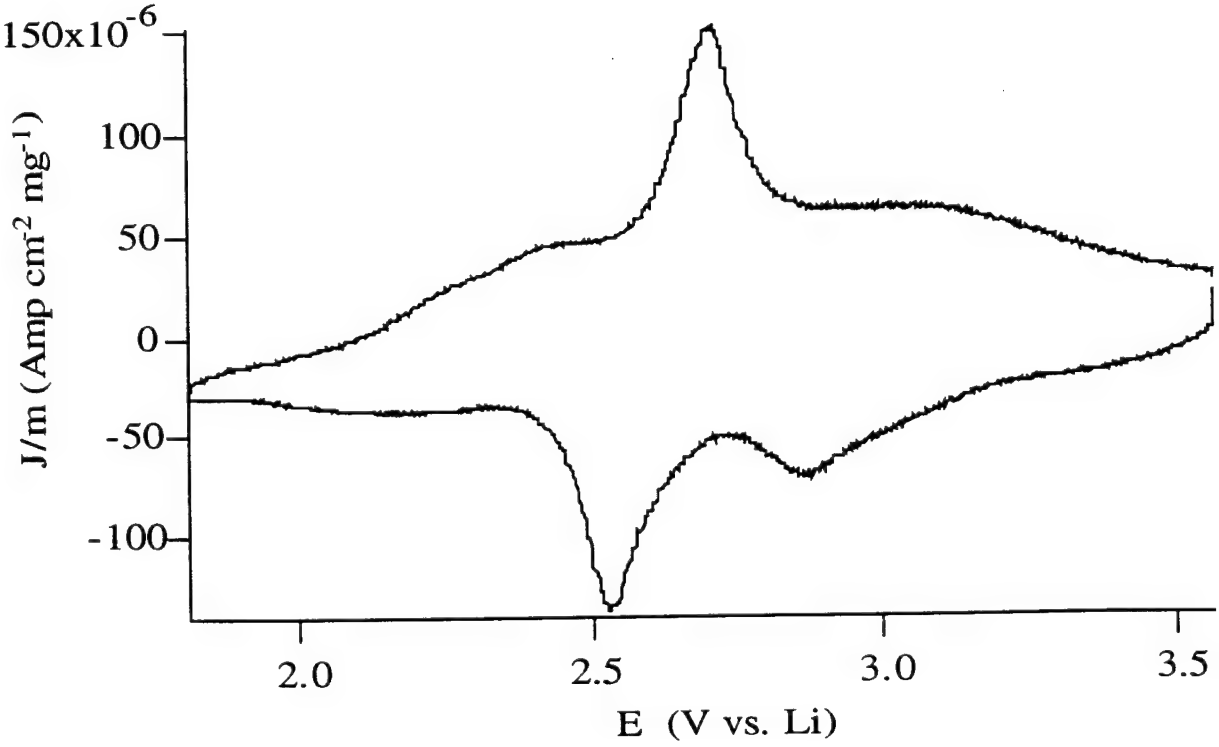
150x10^-6
100
50
0
-50
-100
J/m (Amp cm^-2 mg^-1)
2.0
2.5
3.0
3.5
E (V vs. Li)

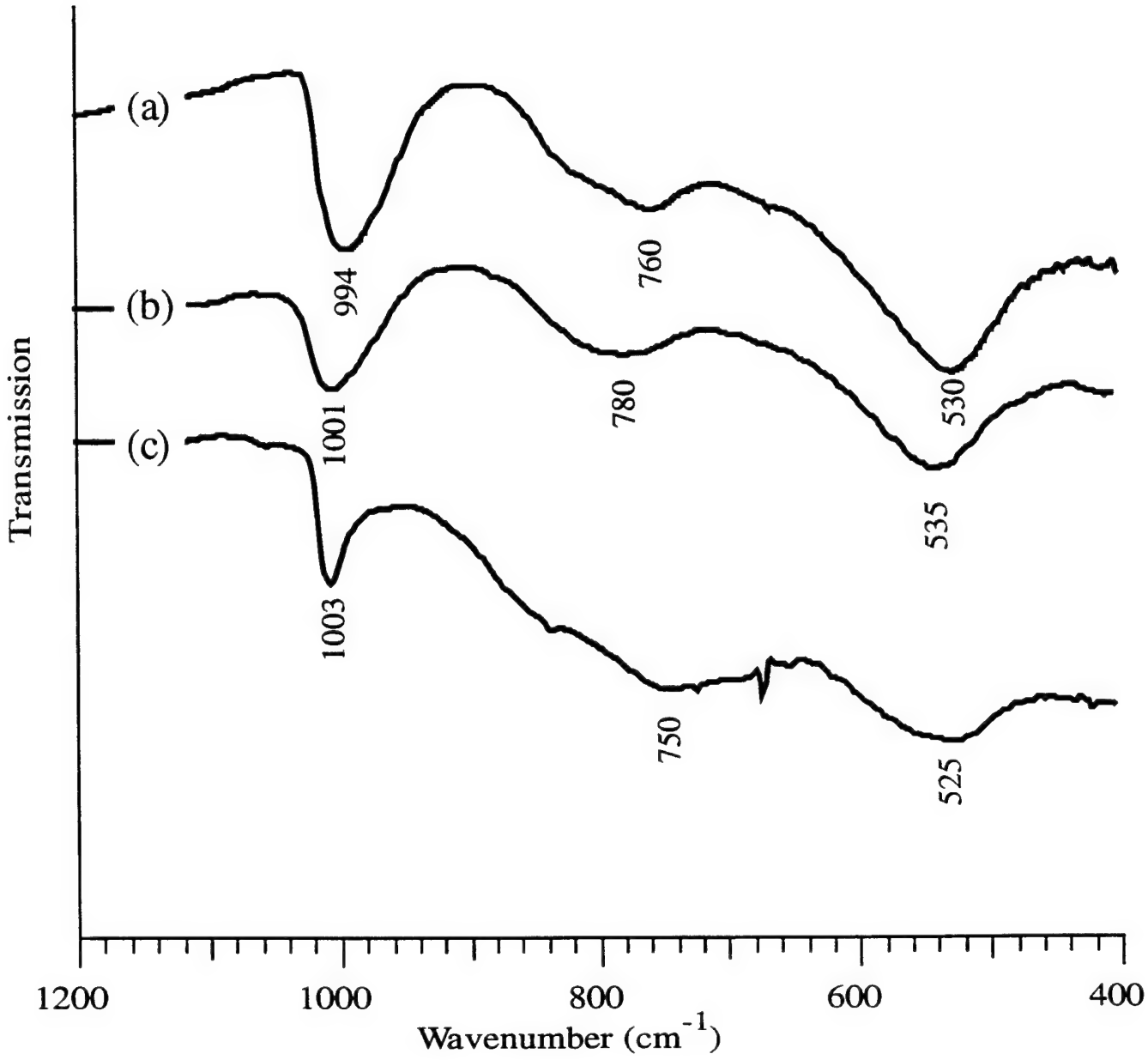
(a)
(b)
(c)
994
760
1001
780
530
535
1003
750
525
Transmission
1200
1000
800
600
400
Wavenumber (cm-1)

(a)

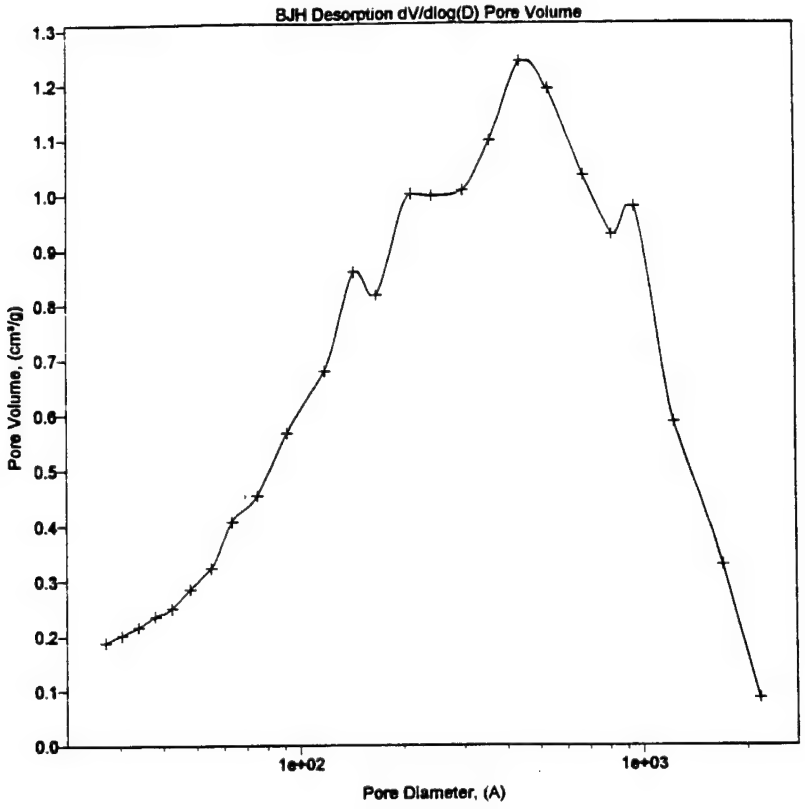
BJH Desorption dV/dlog(D) Pore Volume
Pore Volume, (cm³/g)
1.3
1.2
1.1
1.0
0.9
0.8
0.7
0.6
0.5
0.4
0.3
0.2
0.1
0.0
1e+02
1e+03
Pore Diameter, (A)

(b)

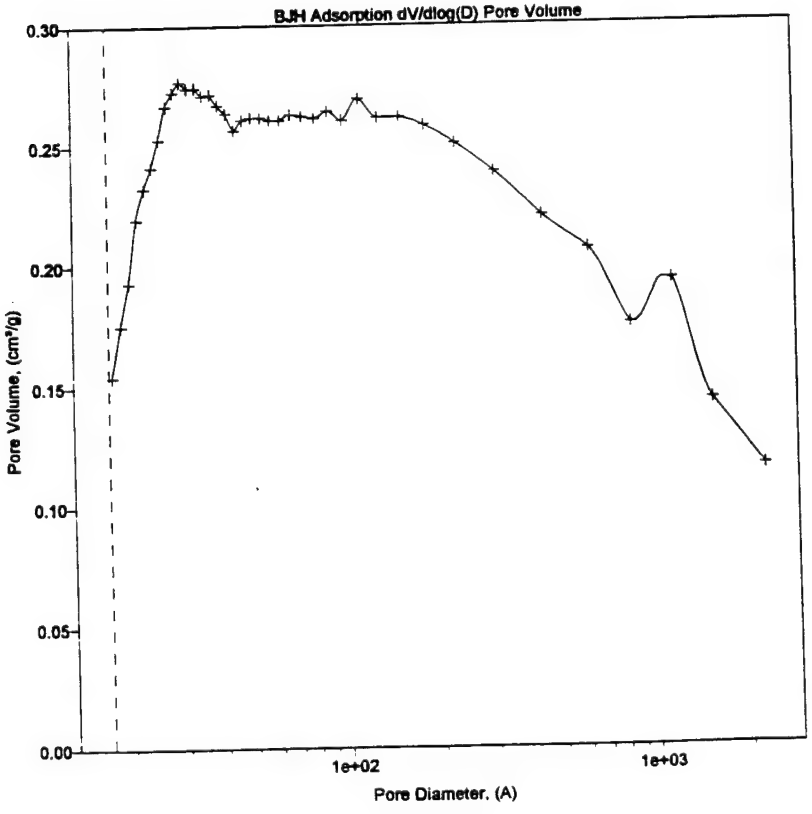
BJH Adsorption dV/dlog(D) Pore Volume
Pore Volume, (cm³/g)
0.30
0.25
0.20
0.15
0.10
0.05
0.00
1e+02
1e+03
Pore Diameter, (A)

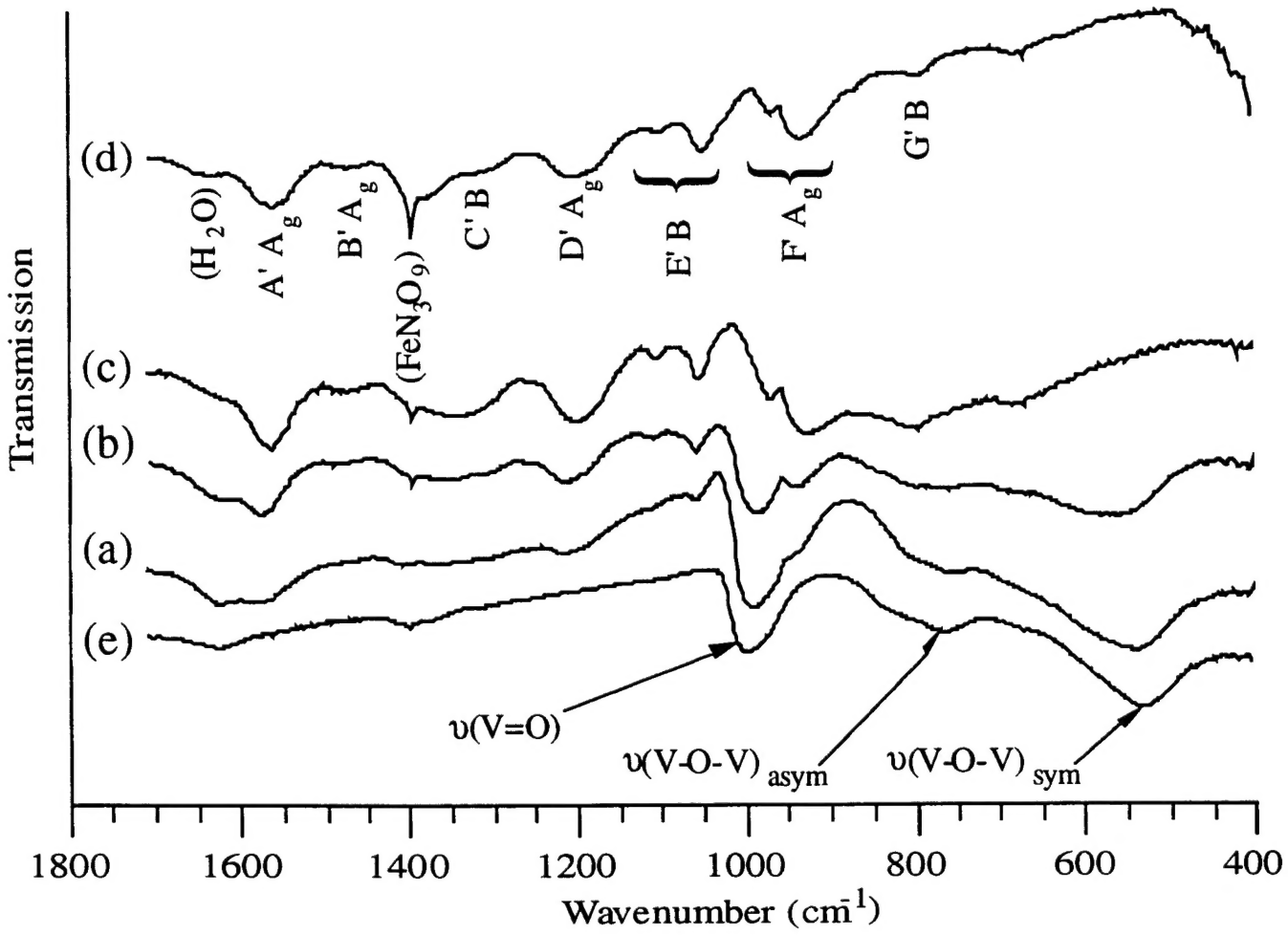
Transmission
(d)
(c)
(b)
(a)
(e)
(H2O)
A' Ag
B' Ag
(FeN3O9)
C' B
D' Ag
E' B
F' Ag
G' B
υ(V=O)
υ(V-O-V) asym
υ(V-O-V) sym
1800
1600
1400
1200
1000
800
600
400
Wavenumber (cm-1)

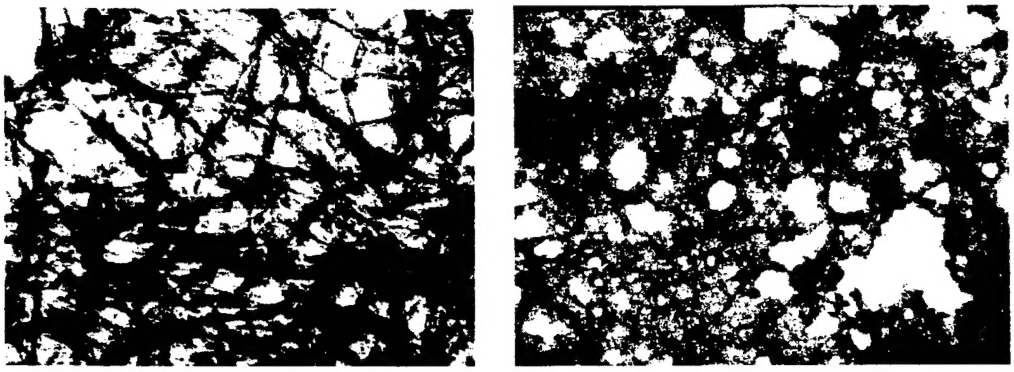
(a)
50 nm
(b)
150 nm

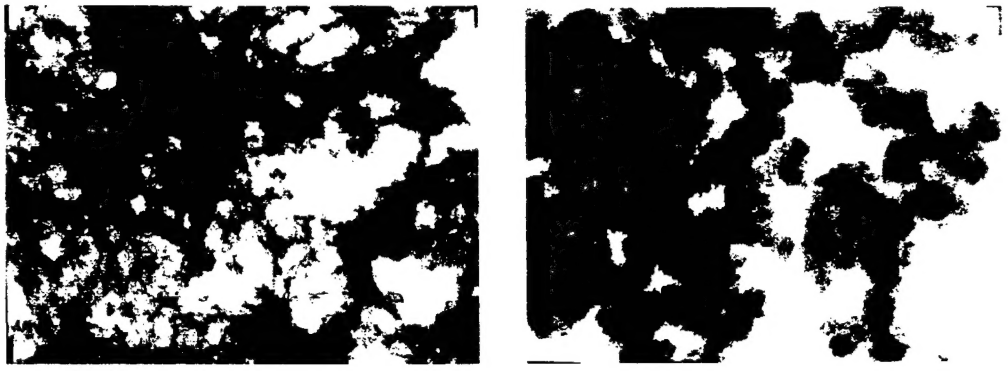
(c)
150 nm
(d)
150 nm

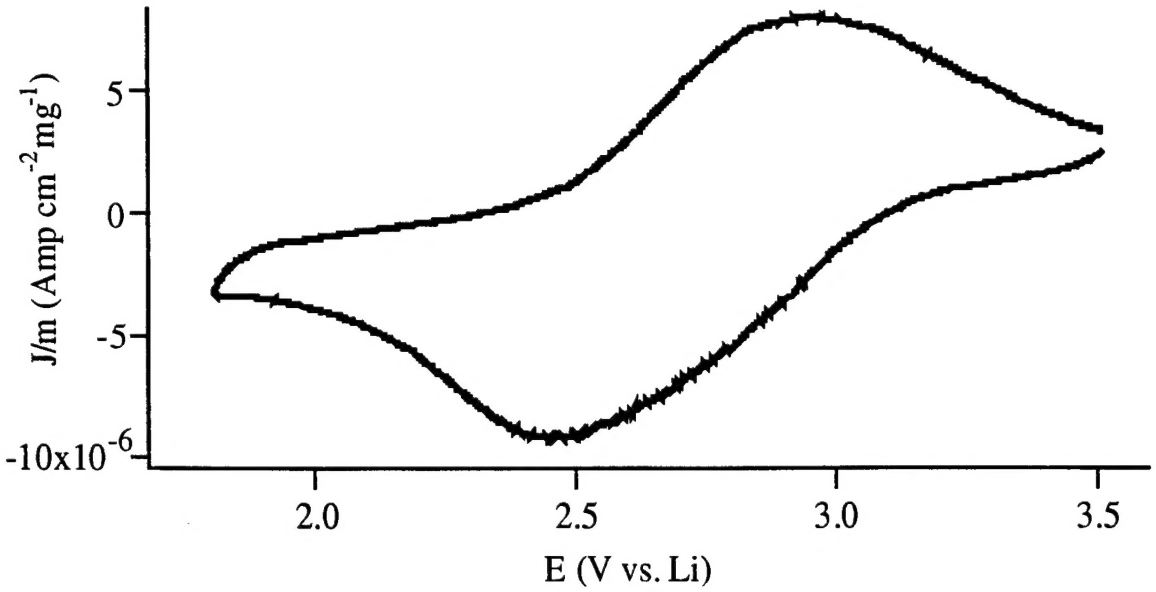
J/m (Amp cm^{-2}mg^{-1})
5
0
-5
-10x10^{-6}
2.0
2.5
3.0
3.5
E (V vs. Li)

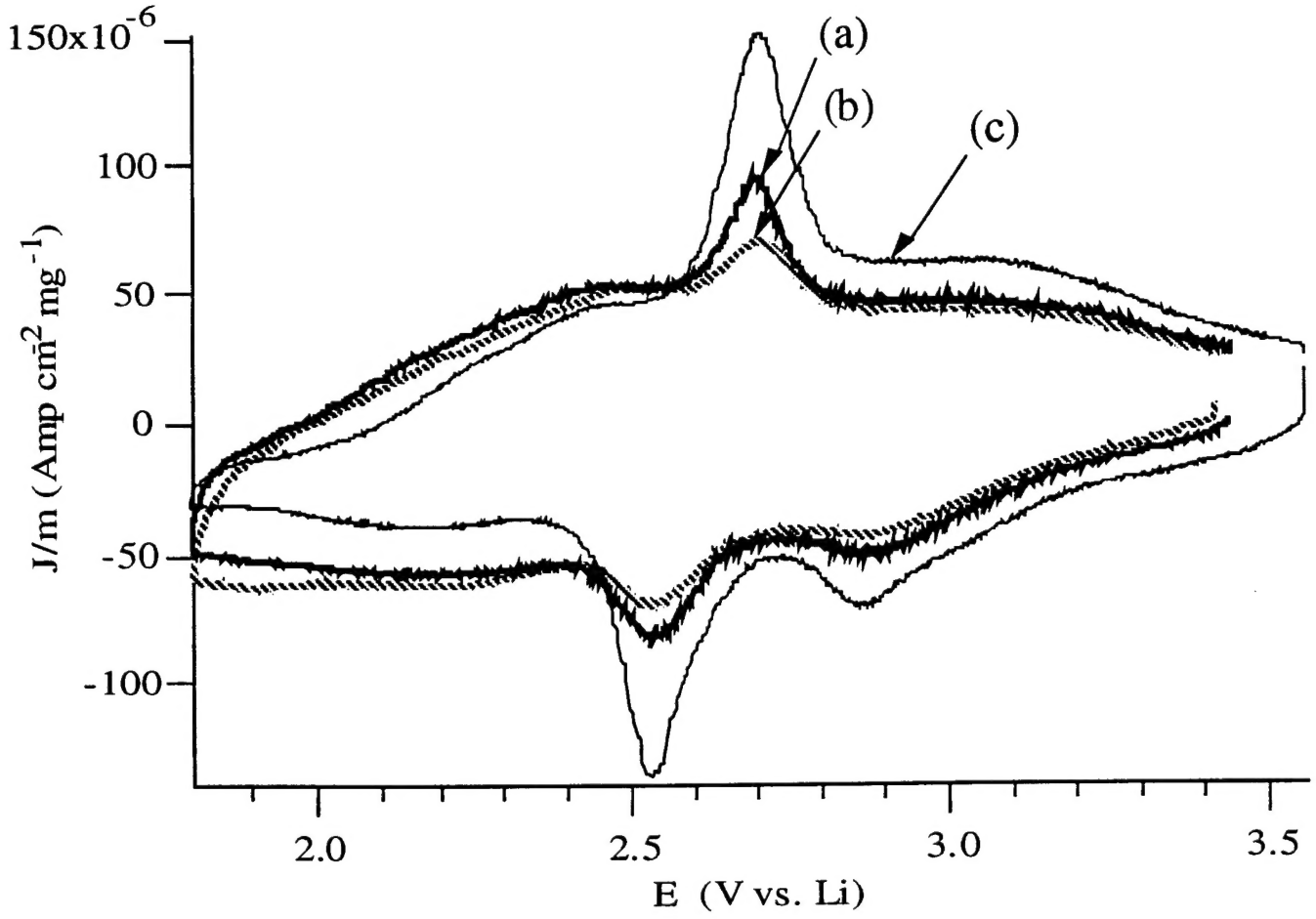
150x10-6
100
50
0
-50
-100
J/m (Amp cm2 mg-1)
(a)
(b)
(c)
2.0
2.5
3.0
3.5
E (V vs. Li)